Coarse-grained molecular dynamics simulation of transport through the nuclear pore complex

Ghavami, Ali

Chapter 4

Studying gel formation properties of disordered nucleoporins

4.1 Introduction

It is widely accepted that the disordered proteins of the nuclear pore complex (NPC) form a selective permeability barrier for all molecules being transported between the cytoplasm and nucleoplasm. They form an efficient barrier for inert molecules larger than $\sim$5 nm in diameter (Mohr et al. 2009, Paine et al. 1975, Keminer and Peters 1999) and facilitate transport for large macromolecules (up to 40 nm in diameter (Lowe et al. 2010)), when they are attached to a transport receptor. The NPC is a large proteinaceous channel with an estimated mass of 44-70 MDa and is composed of approximately 30 different proteins called nucleoporins (Nups). The transport channel of the NPC is lined with several copies of intrinsically disordered proteins that have many phenylalanine-glycine (FG) repeats in their amino acid sequence.

Several models have been proposed to explain the role of the FG-Nups in nuclear transport, but no agreement has been reached yet on a prevalent model (Frey et al. 2006, Rout et al. 2003, Lim et al. 2007, Yamada et al. 2010, Peters 2005, Peters 2009, Wälde and Kehlenbach 2010). One subset of these models is based on the assumption that the interaction between FG-repeats results, effectively, into a "cross-linked" network (a hydrogel) of FG-Nups. The selective phase model presumes that the Kaps can 'melt' through the gel by temporarily breaking the FG-FG cross-links due to their higher affinity to the FG-repeats (compared to the FG-FG affinities). In addition, the space between the cross-links serve as a sieve allowing free diffusion of small molecules, but blocking passage of larger molecules (Frey et al. 2006). Interestingly, none of the other transport models considers FG-repeat cross-linking to play a role in transport.

The gel formation of FG-Nups was first reported for a solution of yeast FG-Nup segments consisting of the N-terminal domain of Nsp1. The transition from the solution (sol) to the gel state had been triggered by lowering the pH of the solution to the physiological pH (Frey et al. 2006). It was shown that an elastic gel is formed at densities higher than 8 mg/mL. In addition, it was demonstrated that FG hydrogels with a sufficiently large concentration of FG-repeat domains form an effective barrier against inert proteins with diameter $\sim$ 7.8 nm (i.e., larger than the permeability limit of the NPC). At the same time, Kap-cargo complexes with the

same size were observed to permeate 1000 times faster into the gel (Frey and Görlich 2007, Mohr et al. 2009).

It has been suggested that the formation of FG hydrogels requires many cohesive units to stabilize the gel through their interactions (Hülsmann et al. 2012). This has been examined by means of mutational analyses showing that F to S mutated Nsp1p FG-Nups were unable to form an elastic hydrogel, even at high concentrations. On the other hand, F to Y mutation did not considerably alter the gel formation properties of Nsp1p yeast nucleoporins (Frey et al. 2006). It has been suggested in further investigations that the interactions that lead to gel formation of FG-Nups are mainly hydrophobic in nature, because mutation of hydrophobic amino acids (i.e., F, L and I) to S prevents the FG-Nups to form a hydrogel (Hülsmann et al. 2012). In addition to experiments, Monte-Carlo simulations on Nsp1p show that the sol-to-gel transition can be driven by hydrophobic interactions (Diesinger and Heermann 2010). However, the effect of the mutations and the electrostatic interactions have not been studied in the simulations.

In this chapter, we will study the gel formation properties of different FG-Nup systems using the developed one-bead-per-amino acid coarse-grained model (see chapter 3). We use percolation theory to identify the sol to gel transition of FG-Nup solutions with different concentrations. We will investigate the effect of FG-repeats on the gelation of FG-Nups by mutating the F residues to hydrophilic and hydrophobic residues. In addition, the critical concentration at which the sol to gel transition occurs is characterized as a function of the charge to hydrophobicity ratio of the amino acid sequence of the FG-Nups.

4.2 Methods

4.2.1 Percolation analysis

When a sol-gel transition occurs, the system transforms from a viscous fluid into an elastic solid (Sahimi 1994). For a polypeptide solution this happens when the concentration exceeds a critical value c_{crit}. At this stage a large interconnected cluster is formed in the system which represents the gel network. The transition from sol to gel can be quantified using percolation theory (Flory 1941).

We have used a finite-size scaling method to determine the critical concentration for an infinite sytem. In this method the percolation probability versus concentration curves $P(c)$ for systems with different sizes are obtained and the intersection of these curves is used to determine c_{crit} (Saven et al. 1991, Wu et al. 2008, Pawłowska and Sikorski 2013) where the percolation probability P is defined as the probability of forming an infinite cluster in the system. The percolation probabilities for different concentrations can be fitted to the function

$$P(c) = 1 - \left(1 + \exp\left(\frac{c-b}{a}\right)\right)^{-1} \tag{4.1}$$

where a and b are fitting constants (Tarasevich and Cherkasova 2007, Adamczyk et al. 2009). The fitting curves are used to quantify the intersection point of the $P(c)$ curves (see Fig. 4.2).

4.2.2 Simulation setup

The Coarse grained simulations are performed using the one-bead-per-amino acid model described in Chapter 3. The FG-Nups are placed in a cubic box of linear size L with periodic boundary conditions and Langevin simulations are performed at 300 K (see Fig. 4.1A). In order to change the concentration of the FG-Nup solutions, the number of FG-Nups, n, is changed while keeping the box size L constant.

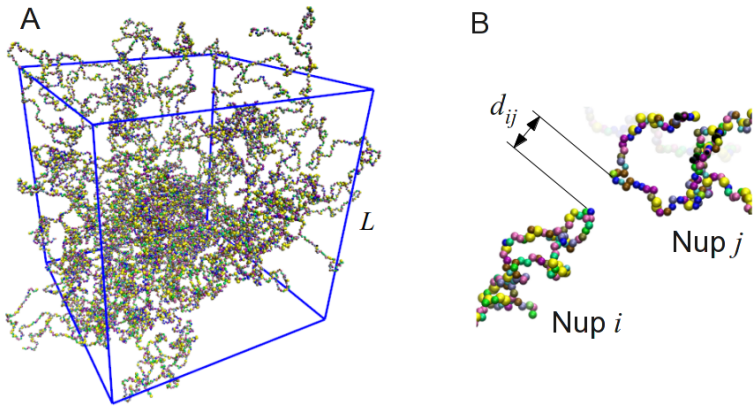

Figure 4.1: A simulation frame ($L = 40$ nm) of an FG-Nup system composed of 38 Nsp1p polypeptides **(A)**. The FG-Nups are colored based on the amino acid type. **(B)** The representation of two FG-Nups in the system and the distance between the Nups.

In order to obtain the percolation probability P, first the connectivity of the FG-Nup network for every simulation frame is analyzed. If at least one residue of two different FG-Nups i and j come closer than a distance $d_{ij} = 0.7$ nm, those Nups are considered to be in contact (see Fig. 4.1B). The choice of 0.7 nm has been made based on the equilibrium distance for hydrophobic interactions $\sigma = 0.6$ nm (see chapter 3) plus 0.1 nm to account for thermal fluctuations around the equilibrium point. A connectivity matrix **C** is then constructed by comparison of all FG-Nups in the system

$$\mathbf{C}_{ij} = \begin{cases} 0 & d_{ij} > 0.7 \text{ nm} \\ 1 & d_{ij} \leq 0.7 \text{ nm} \end{cases} . \tag{4.2}$$

Once the connectivity matrix is constructed, the largest cluster of the system is identified and the maximum dimension of the percolating cluster is calculated in the x, y and z directions. If the maximum dimensions are equal or greater than L, the system is considered to be percolated ($P = 1$) and otherwise the percolation probability P is set to 0. Ultimately, P is calculated by averaging all the percolation probabilities calculated for the different simulation frames. The FG-Nup systems are first energy minimized using a steepest descend method and then simulated for at least 8×10^6 steps and the first 10^6 steps are not considered for the percolation analysis. The percolation probability P is calculated by extracting the coordinates of the

FG-Nups every 10^4 steps. A convergence study on the number of simulation frames required to calculate the percolation probability is shown in Fig. 4.4 of the Appendix which shows that a good accuracy for P can be reached by using 750 simulation frames.

4.3 Results

4.3.1 Network formation properties of FG-Nups

First, the gel formation of a Nsp1p (nsp1 AA 1-606) solution is investigated as was studied by Frey and coworkers (Frey et al. 2006). The average percolation probability versus Nsp1p concentration is calculated and plotted in Fig. 4.2. As expected, larger clusters start to form in the system when the concentration of the FG-Nups in the solution increases. Our results predict a concentration of $c_{\mathrm{crit}} = 27$ mg/mL for the Nsp1p system.

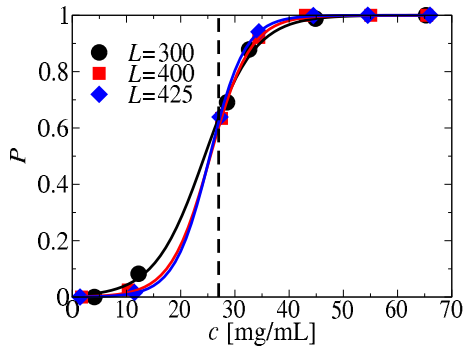

Figure 4.2: The average percolation probability P versus the FG-Nup concentration of the Nsp1p network for three different box sizes L. The intersection of the curves defines the critical density c_{crit}.

4.3.2 The effect of mutations

Next, the effect of mutation of the amino acid sequence of the FG-Nups on the critical concentration is investigated. In the first step, all hydrophobic F residues (hydrophobic strength $\varepsilon_i = 1$, see Table 3.1 of chapter 3) in the amino acid sequence of Nsp1p are replaced with the less hydrophobic S residues ($\varepsilon_i = 0.45$). Our percolation analysis shows that the critical concentration increases to 53 mg/mL for F to S mutated Nsp1p solutions (see Table 4.1 and Fig. 4.5 of the Appendix for the P versus c curves).

On the other hand, the hydrophobic-to-hydrophobic F to Y ($\varepsilon_i = 0.82$) mutation has less effect on the gelation properties of Nsp1p ($c_{\mathrm{crit}} = 38$ mg/mL, see Table 4.1 and Fig. 4.6 of the Appendix). This supports the premise that the cluster formation of the FG-Nups is mainly driven by hydrophobic interactions.

4.3.3 Charge and hydrophobicity effect

The results of the mutated Nsp1p solutions suggest that the hydrophobic interactions are important for the cluster formation in FG-Nups. It can be hypothesized that cluster formation in FG-Nup solutions is promoted by the attractive interaction between hydrophobic amino acids, while in contrast, the repulsive interaction between hydrophilic charged amino acids opposes this effect.

We have investigated this hypothesis by analyzing several FG-Nups with different charge and hydrophobic contents. The hydrophobicity of the FG-Nups is measured by the summation of the hydrophobic strengths ε_i of individual amino acids in the sequence of the FG-Nup, $H = \sum_{j=1}^{N}(\varepsilon_i)$, where N is the total number of amino acids of the FG-Nup (the ε_i values for different amino acids are given in Table 3.1 of chapter 3). Additionally, the charge content of the FG-Nups, C, has been measured by counting the number of charged amino acids in the sequence of the FG-Nups.

It has been show that the critical concentration of polymer solutions depends on the length of the polymers (Adamczyk et al. 2009, Pawłowska and Sikorski 2013). In order to exclude this effect from the results, the charge to hydrophobicity ratio (C/H) for each FG-Nup is normalized by the scaling relation of the gyration radius obtained for disordered proteins in absence of any hydrophobic and electrostatic interaction (see Eq. 1.4). The critical concentrations c_{crit} for several FG-Nup systems has been calculated and plotted against $(C/H)/N^{0.589}$ in Fig. 4.3. The list of the FG-Nup segments and their properties are given in Table 4.1 and the percolation probability versus concentration curves for each FG-Nup are shown in Figs. 4.7 to 4.10 of the Appendix. The results suggest that as the charge to hydrophobicity ratio of the Nups increases, the sol to gel transition occurs at higher concentrations.

FG-Nup Name	Length (AA)	Charge to hydrophobicity ratio C/H	c_{crit} (mg/mL)
Nsp1p	606 (AA 1-606)	0.460	27
Nsp1p F→S	606 (AA 1-606)	0.524	53
Nsp1p F→Y	606 (AA 1-606)	0.484	38
Nsp1n	172 (AA 1-172)	0.035	40
Nup60	151 (AA 389-539)	0.508	58
Nup100s	190 (AA 611-800)	0.539	75
Nup116s	195 (AA 765-960)	0.754	90

Table 4.1: The FG-Nup segments used for the percolation analysis. The selection of Nsp1p is based on the gel formation studies by Frey and coworkers (Frey et al. 2006) and the rest of the FG-Nup segments are selected from (Yamada et al. 2010).

4.4 Discussion and conclusion

The gel formation properties of FG-Nups are investigated by means of a percolation analysis of the conformations of FG-Nup solutions, using a recently developed one-bead-per-amino acid coarse-grained model. The results indicate that a sol to gel transition occurs at $c_{\mathrm{crit}} = 27$ mg/mL for Nsp1p solutions, which is a factor of 3 larger than the experimental critical concentration of 10 mg/mL, based on visual inspection (Frey et al. 2006). Our simulations show

that the critical concentration increases to $c_{\mathrm{crit}} = 53$ mg/mL by mutating all F residues to S in the sequence of Nsp1p. The obtained results are in qualitative agreement with experimental results which have shown that F to S mutated FG-Nup domains fail to form a hydrogel in similar concentrations as the wildtype Nsp1p (Frey et al. 2006, Hülsmann et al. 2012).

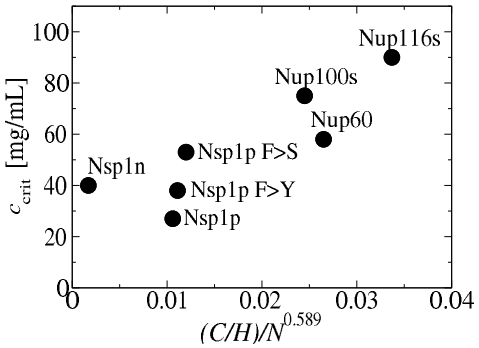

Figure 4.3: The critical concentration c_{crit} for several FG-Nup solutions plotted against the normalized charge to hydrophobicity ratio $(C/H)/N^{0.589}$.

It has been suggested that FG-Nup hydrogels are initially formed through hydrophobic interactions which result into the formation of high molecular weight clusters and are subsequently stabilized by intermolecular hydrogen-bonds (Ader et al. 2010). However, hydrophobic interactions are mentioned to be the main driving force for gel formation of FG-Nups rather than hydrogen bonds, because FG-Nups with mutated hydrophobic residues failed to form a hydrogel (Hülsmann et al. 2012, Ader et al. 2010). Our results on different FG-Nup systems suggest that the critical concentration is related to the charge and hydrophobic content of the FG-Nups. The hydrophobic amino acids contribute to cluster formation through their attractive hydrophobic interactions, while interactions between hydrophilic charged amino acids tend to be repulsive and hence prevent the FG-Nups to form clusters.

Care should be taken in making a direct comparison between the current results and gel formation inside the NPC. Inside the NPC, the FG-Nups are anchored to the scaffold, while in our percolation analysis the FG-Nups are free in solution. In addition, the solutions analyzed here consist of one type of FG-Nups with equal length, while inside the NPC different types of FG-Nups are present, having unequal length. Despite these differences, our results can give several hints about the cluster formation of the FG-Nups inside the NPC. As was shown in chapter 3, the FG-Nups have a non uniform distribution with a low density region at the center of the pore, surrounded by a high density doughnut-like region rich in FG-repeats and a region of mostly charged amino acids near the scaffold of the pore. Comparing the densities of the doughnut-like region with the critical densities of the solutions studied here, suggests that the high density doughnut-like region is prone to form a hydrogel inside the pore. However, further studies are needed to confirm this.

In conclusion, we have investigated the gel formation properties of FG-Nups by using a percolation analysis. Our results confirm that hydrophobic interactions can lead to a sol-gel

transition in FG-Nup solutions. In addition, we show that with increasing charge to hydrophobicity ratio, the critical concentration at which gel formation takes place increases.

4.A Appendix: Convergence study

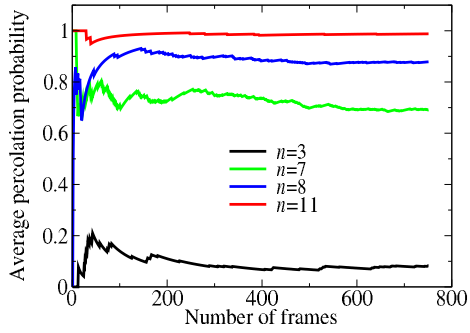

Figure 4.4: Convergence study of the average percolation probability P for Nsp1p with a box size $L = 30$ nm. The lines show the average percolation probability $1/N_{\text{frame}} \sum_{i=1}^{N_{\text{frame}}} P_i$ versus the number of simulation frames N_{frame} for systems with different number of FG-Nups (n).

4.B Appendix: Percolation probability curves

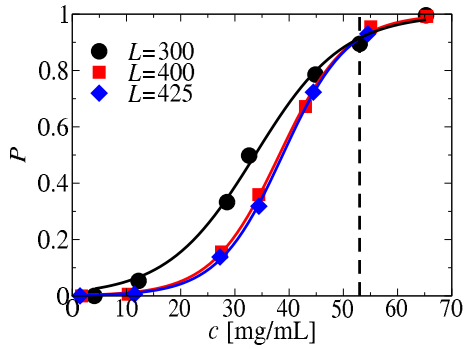

Figure 4.5: The average percolation probability P versus the FG-Nup concentrations for F to S mutated Nsp1p.

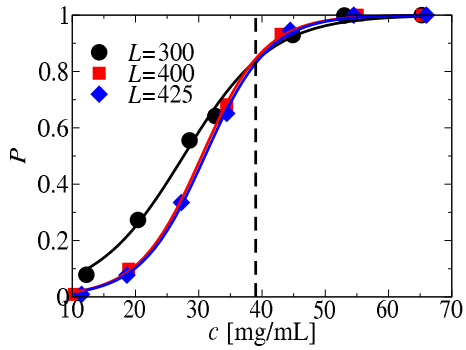

Figure 4.6: The average percolation probability P versus the FG-Nup concentrations for F to Y mutated Nsp1p.

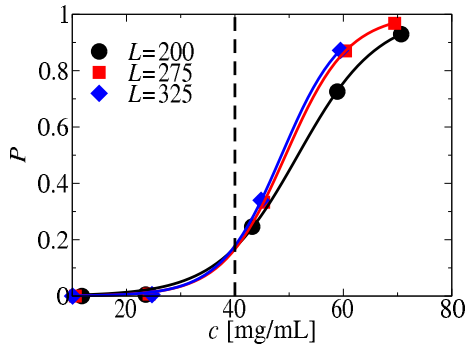

Figure 4.7: The average percolation probability P versus the FG-Nup concentrations for Nsp1n.

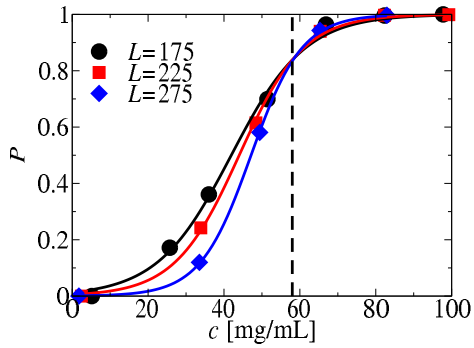

Figure 4.8: The average percolation probability P versus the FG-Nup concentrations for Nup60.

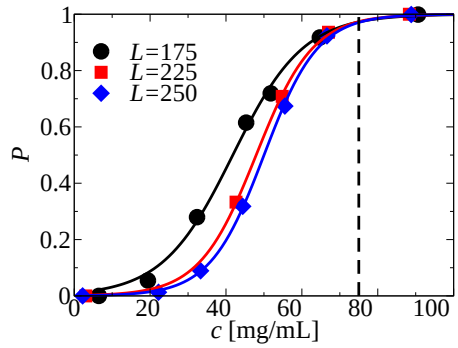

Figure 4.9: The average percolation probability P versus the FG-Nup concentrations for Nup100.

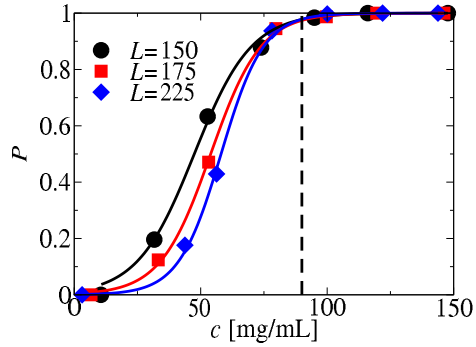

Figure 4.10: The average percolation probability P versus the FG-Nup concentrations for Nup116s.